Stem Cell Research 56 (2021) 102536

Contents lists available at ScienceDirect

Stem Cell Research

journal homepage: www.elsevier.com/locate/scr

Lab Resource: Multiple Cell Lines

Generation of two induced pluripotent stem cell lines with heterozygous and homozygous GAG deletion in TOR1A gene from a healthy hiPSC line

Masuma Akter [a], Haochen Cui [a], Yi-Hsien Chen [b], Baojin Ding [a,*]

[a] Department of Biology, University of Louisiana at Lafayette, 410 East Saint Mary Boulevard, Lafayette LA 70503, USA
[b] Genome Engineering and iPSC Center (GEiC), Washington University at St Louis, MO 63110, USA

A B S T R A C T

A typical DYT1 dystonia is caused by a heterozygous GAG deletion (c.907–909) in the *TOR1A* gene (ΔE, p.Glu303del) and the pathogenesis is not clear. In this study, human induced pluripotent stem cell (hiPSC) lines carrying the heterozygous or homozygous GAG deletion in *TOR1A* gene were generated by genetic modification of a healthy hiPSC line (WTC11, UCSFi001-A). These hiPSC lines showed the normal stem cell morphology and karyotype, expressed the same pluripotency markers as their parental line, and had the capacity to differentiate into three germ layers, providing a valuable resource in determining the pathogenesis of human DYT1 dystonia.

1. Resource Table

Unique stem cell lines identifier	ULLi002-A-49 ULLi002-A-51
Institution	University of Louisiana at Lafayette, LA USA
Contact information of the reported cell line distributor	Baojin Ding (Baojin.Ding@Louisiana.edu)
Type of cell lines	iPSC
Origin	Human
Additional origin info *(applicable for human ESC or iPSC)*	Age: 30 YR Sex: Male Ethnicity: Asian
Cell Source	Skin fibroblasts.
Method of reprogramming	N/A
Clonality	Clonal
Evidence of the reprogramming transgene loss (including genomic copy if applicable)	RT/q-PCR
Cell culture system used	Serum-free and feeder-free medium
Type of Genetic Modification	Induced mutation
Associated disease	DYT1 dystonia
Gene/locus	TOR1A c.907_909delGAG (p.Glu303del)/ 9q34.11
Multiline rationale	Isogenic clones carrying heterozygous or homozygous of the same gene mutation.
Method of modification/site-specific nuclease used	CRISPR/Cas9
Site-specific nuclease (SSN) delivery method	Electroporated with a 4D-Nucleofector (Lonza) using CA-137 program.
All genetic material introduced into the cells	gRNA vector MLM3636 (Addgene #43860) Cas9 vector p3s-Cas9HC (Addgene #43945)

(*continued on next column*)

(*continued*)

Unique stem cell lines identifier	ULLi002-A-49 ULLi002-A-51
Analysis of the nuclease-targeted allele status	Sequencing of the targeted allele
Method of the off-target nuclease activity surveillance	Targeted PCR/sequencing
Name of transgene	N/A
Eukaryotic selective agent resistance (including inducible/gene expressing cell-specific)	N/A
Inducible/constitutive system details	N/A
Date archived/stock date	4/29/2021
Cell line repository/bank	https://hpscreg.eu/cell-line/ULLi002-A-49 https://hpscreg.eu/cell-line/ULLi002-A-51
Ethical/GMO work approvals	Genetic modification was performed at Genome Engineering and iPSC Center (GEiC) at Washington University in St. Louis.
Addgene/public access repository recombinant DNA sources' disclaimers (if applicable)	N/A

2. Resource utility

Although rodent models of DYT1 dystonia provide insights into disease mechanisms, significant species-dependent differences exist because animals with the identical heterozygous mutation fail to show pathology. These hiPSC lines will provide a valuable resource to develop human cellular systems in modeling DYT1 dystonia. Table 1

* Corresponding author.
E-mail address: Baojin.Ding@Louisiana.edu (B. Ding).

https://doi.org/10.1016/j.scr.2021.102536
Received 19 May 2021; Received in revised form 19 August 2021; Accepted 6 September 2021
Available online 11 September 2021

3. Resource details

Dystonia is a common movement disorder characterized by sustained or intermittent muscle contractions causing abnormal movements and/or postures. Because the clinical characteristics and underlying causes of dystonia are very heterogeneous, the pathological mechanisms of dystonia remain largely unknown (Ding, 2022). The diagnosis and etiological definition of this disorder remain challenging. The childhood-onset DYT1 dystonia represents the most frequent and severe form of dystonia, providing an excellent example to understand the pathogenesis of this disease. The typical DYT1 dystonia is caused by a heterozygous GAG deletion (c.907–909) in the *TOR1A* gene (ΔE, p. Glu303del) (Ozelius et al., 1997). Interestingly, mice with the identical *Tor1a* mutation as a heterozygote failed to show any pathological phenotypes (Goodchild et al., 2005), suggesting that the significant species-dependent differences exist between DYT1 mouse models and human patients. However, the limited access to patient neurons and the lack of *in vitro* human neuronal systems greatly impede the progress of research in dystonia. Generation of hiPSC lines containing disease-causing mutations and their isogenic controls has been shown to be a powerful tool in modeling human neurological diseases (Sepehrimanesh and Ding, 2020; Ding et al., 2021). In this study, we genetically modified a well-characterized hiPSC line (WTC11, UCSFi001-A) with CRISPR/Cas9 method and obtained two iPSC clones carrying the heterozygous (ULLi002-A-49, or USCFi001-A-49) and homozygous (ULLi002-A-51, or USCFi001-A-51) GAG deletion in the *TOR1A* gene, respectively. These hiPSC lines and their isogenic controls provide a valuable resource in modeling DYT1 dystonia.

Both lines showed a typical pluripotent stem cell morphology with a high nucleus/cytoplasm ratio (Fig. 1A). Sanger DNA sequencing of polymerase chain reaction (PCR) products (Fig. 1B) and deep sequencing analysis (Supp. Fig. S1A and S1B) confirmed that these iPSC lines contain heterozygous (ULLi002-A-49) and homozygous (ULLi002-A-51) GAG deletion (c.907–909) in the *TOR1A* gene. Chromosomes from iPSCs were harvested and analyzed using the GTW banding method. Of 20 metaphase cells examined of each clone, all cells are characteristic of a chromosomally normal male karyotype, 46, XY (Fig. 1C). Short tandem repeat (STR) analysis at 18 loci indicated that ULLi002-A-49 and ULLi002-A-51 clones completely matched the parental hiPSC (UCSFi001-A) identity (Supp. Fig. S1C). Immunostaining indicated that these iPSCs highly expressed pluripotency markers of *OCT4, NANOG, SOX2,* and *SSEA4* (Fig. 1D). Quantitative RT-PCR analysis demonstrated that the pluripotency markers of *OCT4*, SOX2, *NANOG*, and *KLF4* were expressed at similar levels as their parental line (UCSFi001A) (Fig. 1F). Following spontaneous differentiation, embryoid bodies (EBs) (Fig. 1E) derived from ULLi002-A-49 and ULLi002-A-51 displayed dramatic upregulation of markers of the ectoderm (*PAX6, OTX1*), mesoderm (*DCN, IGF2, GATA2*) and endoderm (*SOX7, SOX17)* lineages. The expression levels of these trilineage markers were consistent with their parental line UCSFi001-A and much higher than undifferentiated iPSCs (Fig. 1G). PCR screening demonstrated that ULLi002-A-49 and ULLi002-A-51 were negative for mycoplasma (Fig. S1 D).

4. Materials and methods

4.1. Generate and culture TOR1A mutant iPSCs

Human *TOR1A* mutant clones were generated from the WTC11 iPSC line (Gladstone institute, UCSFi001-A) by the Genome Engineering and iPSC center (GEiC) at Washington University in St. Louis. Briefly, approximately 1×10^6 single cells were resuspended in P3 primary buffer (Lonza) with gRNA/Cas9 ribonucleoprotein (RNP) complex (200 pmol synthetic gRNA and 80 pmol SpCas9 protein) and hTOR1A mutant single-stranded oligo donor (ssODN) (Table 2). Subsequently, cells were

Table 1
Characterization and validation.

Classification	Test	Result	Data
Morphology	Photography	Typical primed pluripotent human stem cell morphology.	Fig. 1 Panel A
Pluripotency status evidence for the described cell line	Qualitative analysis	Immunocytochemistry showed expression of pluripotency markers: OCT4, SOX2, NANOG, SSEA4.	Fig. 1 Panel D
	Quantitative analysis	Compared to DAPI, % of positive cell (ULLi002-A-49, ULLi002-A-51) OCT4: 98%, 98%; SOX2: 99%, 98%; NANOG: 97%, 95%; SSEA-4: 97%, 98%. RT-PCR showed highly express OCT4, SOX2, NANOG, KLF4.	Fig. 1 Panel D and F
Karyotype	Karyotype (G-banding) and resolution	46, XY, Resolution 400	Fig. 1 Panel C
Genotyping for the desired genomic alteration/allelic status of the gene of interest	PCR across the edited site and deep sequencing analysis	Heterozygous or homozygous GAG deletion (c.907–909) in *TOR1A* gene.	Fig. 1 Panel B and Supplementary Fig. S1A and B.
	Transgene-specific PCR	N/A	N/A
Verification of the absence of random plasmid integration events	PCR/Southern	Off Target Analysis of gRNA showed 100% minus a weighted sum of off-target hit-scores in the target genome.	N/A
Parental and modified cell line genetic identity evidence	STR analysis, microsatellite PCR (mPCR) or specific (mutant) allele seq	STR analysis of 18 loci, all matched.	Supplementary Fig. S1C
Mutagenesis/genetic modification outcome analysis	Sequencing (genomic DNA PCR or RT-PCR product)	The sequencing results of genomic DNA all matched with the parental line.	Fig. 1 Panel B and Supplementary Fig. S1A and B
	PCR-based analyses	The sequencing results PCR products all matched with the parental line.	Fig. 1 Panel B and Supplementary Fig. S1A and B
	Southern Blot or WGS; western blotting (for knock-outs, KOs)	N/A	N/A
Off-target nuclease analysis	PCR across top 5/10 predicted top likely off-target sites, whole genome/exome sequencing	N/A	N/A
Specific pathogen-free status	Mycoplasma	Tested by MycoAlert PLUS kit: Negative	Fig. S1D
Multilineage differentiation potential	Embryoid body formation, RT-PCR	Upregulation of trilineage markers *PAX6, OTX1* (ectoderm), *DCN, IGF2, GATA2* (mesoderm), and *SOX7, SOX17* (endoderm).	Fig. 1 Panel G
Donor screening (OPTIONAL)	HIV 1 + 2 Hepatitis B, Hepatitis C	N/A	N/A
Genotype additional info (OPTIONAL)	Blood group genotyping	N/A	N/A
	HLA tissue typing	N/A	N/A

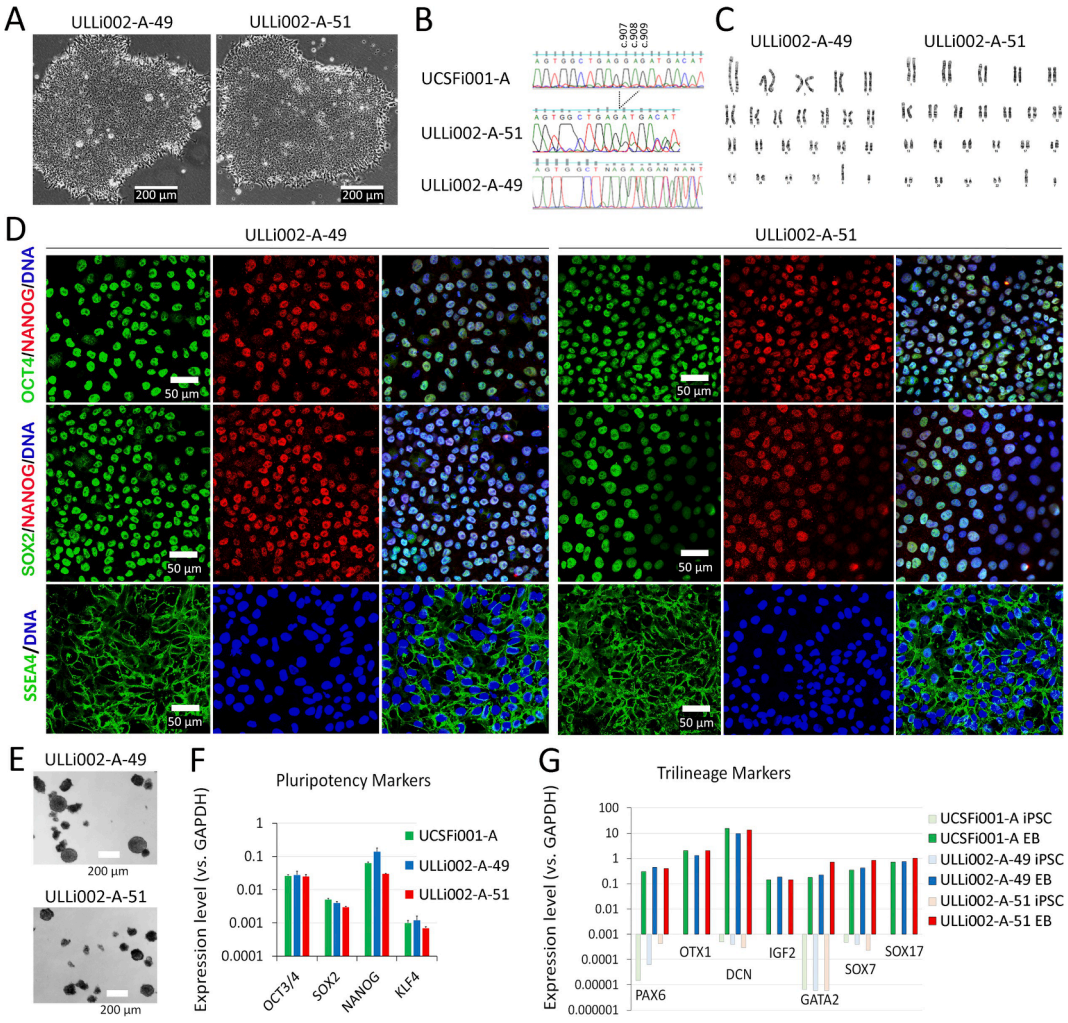

Fig. 1. Characterization of ULLi002-A49 and ULLi002-A51 iPSC lines.

electroporated with a 4D-Nucleofector (Lonza) using CA-137 program. Following nucleofection, the editing efficiency was confirmed by targeted deep sequencing using primer sets specific to target regions, and then the pool was single-cell sorted. Single cell clones were screened with targeted deep sequencing analysis. All iPSCs were cultured with mTeSR Plus (STEMCELL Technology) on matrigel-coated plates at 37 °C in a humidified, 5% CO2 incubator and passage at a 1:6 ratio using gentle cell dissociation reagent (Versene, Gibco).

4.2. Embryoid bodies (EB) formation

hiPSCs were dissociated with Versene and transferred to low attachment 10-cm petri dishes in KOSR medium (DMEM/F12 medium containing 20% KnockOut Serum Replacement, 1% GlutaMax, 1% non-essential amino acids, 50 µM β-mercaptoethanol, and 1% penicillin–streptomycin) supplemented with 10 µM Y-27632. The medium was changed every other day and EBs gradually formed. After 7 days of suspension culture, EBs were digested with 0.25% Trypsin and cultured on gelatin coated plates with KOSR medium for another 7 days. The total RNAs were extracted for RT-PCR analysis.

4.3. Immunostaining and confocal microscopy

Briefly, cultured iPSCs were fixed with 4% paraformaldehyde (PFA) in PBS for 15 min at room temperature followed by incubation in blocking buffer (3% bovine serum albumin in PBS) with (for nuclear markers) or without (for cell surface marker SSEA4) 0.2% Triton X-100 for 1 h. Cells were then incubated with primary antibodies (Table 2) in blocking buffer at 4 °C overnight and then followed by washing and incubation with fluorophore-conjugated corresponding secondary antibodies at room temperature for 2 hrs. Nuclei were stained with Hoechst 33342 (Invitrogen). Images were obtained with a Leica SP5 confocal microscope.

4.4. Quantitative PCR analysis

iPSCs and EBs were collected from cultured plates and lysed in TRIzol (Invitrogen). Total RNAs were isolated by the phenol/chloroform extracting method, and then were reverse-transcribed into cDNAs with the SuperScript™ III Reverse Transcriptase (Invitrogen). Quantitative PCR analysis was performed using SYBR Green PCR Master Mix (Applied Biosystems) and run on StepOne qPCR machine (Applied Biosystems). The gene expression data were analyzed using the $\Delta\Delta C_T$ method and the values were normalized to the expression of the GAPDH housekeeping gene (Fig. 1F and G). Primers used in this study were listed in Table 2.

4.5. Karyotyping

Chromosomes from iPSC clones were analyzed using the GTW banding method at GEiC at Washington University in St. Louis.

Table 2
Reagents details.

Antibodies used for immunocytochemistry			
	Antibody	Dilution	Company Cat # and RRID
Pluripotency Markers	Mouse anti-OCT4	1:200	Santa Cruz Cat# sc-5279, RRID: AB_628051
	Mouse anti-SOX2	1:200	Santa Cruz Biotechnology Cat# sc-365823, RRID:AB_10842165
	Mouse anti-SSEA4	1:200	Abcam Cat# ab16287, RRID:AB_778073
	Rabbit anti-Nanog	1:100	Abcam Cat# ab21624, RRID:AB_446437
Secondary antibodies	Donkey anti-Mouse IgG (H + L), Alexa Fluor 488	1:500	Jackson ImmunoResearch Labs Cat# 715-545-150, RRID:AB_2340846
	Donkey Anti-Rabbit IgG (H + L), Alexa Fluor 594	1:500	Jackson ImmunoResearch Labs Cat# 711-585-152, RRID:AB_2340621
Nuclear stain	Hoechst33342	1 μg/mL	Invitrogen Cat # H3570. RRID: NOT FOUND
Site-specific nuclease			
Nuclease information	Cas9	Cas9 vector p3s-Cas9HC (Addgene #43945)	
Delivery method	electroporation	4D-Nucleofector (Lonza, Cat # AAF-1002B)	
Selection/enrichment strategy	sorted into 96-well plates with one cell per well	Single cell clones were screened and expanded	
Primers and Oligonucleotides used in this study			
	Target	Forward/Reverse primer (5′-3′)	
Pluripotency marker	OCT 3/4	CGAGAGGATTTTGAGGCTGC/CGAGGAGTACAGTGCAGTGA	
Pluripotency marker	SOX 2	AGGATAAGTACACGCTGCCC/TTCATGTGCGCGTAACTGTC	
Pluripotency marker	NANOG	TGTCTTCTGCTGAGATGCCT/CAGAAGTGGGTTGTTTGCCT	
Pluripotency marker	KLF4	TCTCCAATTCGCTGACCCAT/CGGATCGGATAGGTGAAGCT	
Differentiation marker	PAX6	GGGCGGAGTTATGATACCTACA/ATATCAGGTTCACTTCCGGGAA	
Differentiation marker	OTX1	TACGCCCTCCTCTTCCTACT/GCATGTGGGTGGTGATGATG	
Differentiation marker	DCN	CTGAAGAACCTTCACGCATTGA/GGCAATTCCTTCAGCTGATTCT	
Differentiation marker	IGF2	CAATATGACACCTGGAAGCAGT/GTAGAGCAATCAGGGGACGG	
Differentiation marker	GATA2	ACCTGTTGTGCAAATTGTCAGA/ATCCCTTCCTTCTTCATGGTCA	
Differentiation marker	SOX7	ACTCCACTCCAACCTCCAAG/TTCATTGCGATCCATGTCCC	
Differentiation marker	SOX17	ATCGGGGACATGAAGGTGAA/TCCTTAGCCCACACCATGAA	
House-Keeping Genes	GAPDH	CAAATTCCATGGCACCGTCA/GGACTCCACGACGTACTCAG	
Genotyping-PCR	TOR1A	ACAGCAGCTTAATTGACCGGA/ATCATGAGCCCTGCGATGAG	
Sequencing	TOR1A	GTGTATCCGAGTGGAAATGC	
hTOR1A gRNA (IDT)	TOR1A	TGAAGACATTGTAAGCAGAG	
hTOR1A ssODN (IDT)	TOR1A	AATGTGTATCCGAGTGGAAATGCAGTCCCGAGGCTATGAAATT GATGAAGACATTGTAAGTAGAGTGGCTGAGATGACATTTTTCC CCAAAGAGGAGAGAGTTTTCTCAGATAAAGGCTGCA	

4.6. STR analysis

Short tandem repeat (STR) analysis of 18 loci (Fig. S1C) were performed at GEiC at Washington University in St. Louis.

4.7. Mycoplasma test

Mycoplasma test (Fig. S1D) was performed by MycoAlert PLUS kit (Lonza) at GEiC at Washington University in St. Louis.

Declaration of Competing Interest

The authors declare that they have no known competing financial interests or personal relationships that could have appeared to influence the work reported in this paper.

Acknowledgements

We thank Genome Engineering & iPSC Center (GEiC) at Washington University in St. Louis for their excellent services, and members of the Ding laboratory (Dr. Masood Sepehrimanesh, Mr. Jacob Stagray, Mr. Casey Coutee, and Mr. Md Abir Hosain) for help and discussion. This work was supported by National Institute of Neurological Diseases and Stroke (No. NIH/NINDS NS112910 to B.D.) and Department of Defense (DoD) Peer Reviewed Medical Research Program (PRMRP) Discovery Award (No. W81XWH2010186 to B.D.).

Appendix A. Supplementary data

Supplementary data to this article can be found online at https://doi.org/10.1016/j.scr.2021.102536.

References

Ding, B., 2022. Novel insights into the pathogenesis of DYT1 dystonia from induced patient-derived neurons. Neural Regen Res 17 (3), 561. https://doi.org/10.4103/1673-5374.320978.

Ding, B., Tang, Y.u., Ma, S., Akter, M., Liu, M.-L., Zang, T., Zhang, C.-L., 2021. Disease Modeling with Human Neurons Reveals LMNB1 Dysregulation Underlying DYT1 Dystonia. J Neurosci 41 (9), 2024–2038.

Goodchild, R.E., Kim, C.E., Dauer, W.T., 2005. Loss of the dystonia-associated protein torsinA selectively disrupts the neuronal nuclear envelope. Neuron 48 (6), 923–932.

Ozelius, L.J., Hewett, J.W., Page, C.E., Bressman, S.B., Kramer, P.L., Shalish, C., de Leon, D., Brin, M.F., Raymond, D., Corey, D.P., Fahn, S., Risch, N.J., Buckler, A.J., Gusella, J.F., Breakefield, X.O., 1997. The early-onset torsion dystonia gene (DYT1) encodes an ATP-binding protein. Nat Genet 17 (1), 40–48.

Sepehrimanesh, M., Ding, B., 2020. Generation and Optimization of Highly Pure Motor Neurons from Human Induced Pluripotent Stem Cells via Lentiviral Delivery of Transcription Factors. Am J Physiol Cell Physiol 319 (4), C771–C780.